



THE UNIVERSITY *of* EDINBURGH

Edinburgh Research Explorer

Aberrant subcutaneous adipogenesis precedes adult metabolic dysfunction in an ovine model of polycystic ovary syndrome (PCOS)

Citation for published version:

Siemienowicz, KJ, Coukan, F, Franks, S, Rae, N & Duncan, WC 2021, 'Aberrant subcutaneous adipogenesis precedes adult metabolic dysfunction in an ovine model of polycystic ovary syndrome (PCOS)', *Molecular and Cellular Endocrinology*, vol. 519, no. 1, 111042.
<https://doi.org/10.1016/j.mce.2020.111042>

Digital Object Identifier (DOI):

[10.1016/j.mce.2020.111042](https://doi.org/10.1016/j.mce.2020.111042)

Link:

[Link to publication record in Edinburgh Research Explorer](#)

Document Version:

Peer reviewed version

Published In:

Molecular and Cellular Endocrinology

General rights

Copyright for the publications made accessible via the Edinburgh Research Explorer is retained by the author(s) and / or other copyright owners and it is a condition of accessing these publications that users recognise and abide by the legal requirements associated with these rights.

Take down policy

The University of Edinburgh has made every reasonable effort to ensure that Edinburgh Research Explorer content complies with UK legislation. If you believe that the public display of this file breaches copyright please contact openaccess@ed.ac.uk providing details, and we will remove access to the work immediately and investigate your claim.



1 **Title: Aberrant subcutaneous adipogenesis precedes adult metabolic**
2 **dysfunction in an ovine model of polycystic ovary syndrome (PCOS)**

3

4 **Authors:** Katarzyna J. Siemienowicz^{a,b*}, Flavien Coukan^b, Stephen Franks^c, Mick
5 T. Rae^b, W. Colin Duncan^a

6

7 **Affiliations:** ^aMRC Centre for Reproductive Health, The University of Edinburgh,
8 Edinburgh EH16 4TJ, UK; ^bSchool of Applied Sciences, Edinburgh Napier University,
9 Edinburgh EH11 4BN, UK; ^cInstitute of Reproductive and Developmental Biology,
10 Imperial College, London, UK.

11

12 ***Corresponding Author:**

13 Katarzyna J. Siemienowicz
14 School of Applied Sciences,
15 Edinburgh Napier University,
16 Edinburgh EH11 4BN, UK

17 **Tel:** +44 (0)131 455 3458

18 **E-mail:** k.siemienowicz@napier.ac.uk

19

20 **Abstract**

21 Polycystic ovary syndrome (PCOS) affects over 10% of women. Insulin resistance,
22 elevated free fatty acids (FFAs) and increased adiposity are key factors contributing
23 to metabolic dysfunction in PCOS. We hypothesised that aberrant adipogenesis
24 during adolescence, and downstream metabolic perturbations, contributes to the
25 metabolic phenotype of adult PCOS. We used prenatally androgenized (PA) sheep as
26 a clinically realistic model of PCOS. During adolescence, but not during fetal or early
27 life of PA sheep, adipogenesis was decreased in subcutaneous adipose tissue (SAT)
28 accompanied by decreased leptin, adiponectin, and increased FFAs. In adulthood, PA
29 sheep developed adipocyte hypertrophy in SAT paralleled by increased expression of
30 inflammatory markers, elevated FFAs and increased expression of genes linked to fat
31 accumulation in visceral adipose tissue. This study provides better understanding into
32 the pathophysiology of PCOS from puberty to adulthood and identifies opportunity for
33 early clinical intervention to normalise adipogenesis and ameliorate the metabolic
34 phenotype.

35

36 **Keywords:** polycystic ovary syndrome, adipose tissue, adipogenesis, prenatal
37 programming, metabolism, androgens

38

39 **1. Introduction**

40 Polycystic ovary syndrome (PCOS) is a common disorder, affecting up to 10% of
41 women of reproductive age (Fauser et al., 2012). Women with PCOS have increased
42 risks of hyperinsulinemia, insulin resistance, obesity, dyslipidemia and fatty liver
43 (Fauser et al., 2012; Moran et al., 2015; Teede et al., 2010). Metabolic comorbidities
44 associated with the syndrome worsen with age and pose a significant health and
45 economic burden (Jason, 2011; Teede et al., 2010).

46 Overweight/obese women with PCOS have increased abdominal adiposity when
47 compared with BMI-matched controls, correlated with an adverse metabolic profile
48 (Puder et al., 2005; Yildirim et al., 2003). In addition, women with PCOS have
49 adipose tissue dysfunction, independent of obesity (Carmina et al., 2005; Echiburú et
50 al., 2018; Manneras-Holm et al., 2010; Seow et al., 2009; Wang et al., 2012).

51 Although studies using animal models of PCOS have also indicated adipose tissue
52 abnormalities, the data is inconclusive (Keller et al., 2014; Puttabyatappa et al.,
53 2018; Veiga-Lopez et al., 2013). Insulin and androgens, both typically increased in
54 PCOS, affect adipogenesis and adipose tissue function (Chazenbalk et al., 2013;
55 Klemm et al., 2001), and thus are likely to play an important role in adipose tissue
56 dysfunction in PCOS. White adipose tissue (WAT) is a key metabolic and endocrine
57 organ regulating energy homeostasis, insulin sensitivity and inflammation, therefore
58 functional WAT is essential in maintaining body homeostasis (Lafontan, 2014). There
59 is strong evidence showing differences between subcutaneous adipose tissue (SAT)
60 and visceral adipose tissue (VAT) biology, including distinct gene expression in VAT
61 and SAT preadipocytes (Macotela et al., 2012; Tchkonina et al., 2013)

62 Animal models of PCOS are instrumental in dissecting mechanisms underlying the
63 pathophysiology of PCOS (Abbott et al., 2013; Padmanabhan and Veiga-Lopez,

64 2013). We have previously documented that ewes exposed to increased androgens
65 *in utero* manifest ovarian, hormonal and metabolic phenotypes reminiscent of PCOS
66 (Hogg et al., 2011; 2012; Rae et al., 2013; Ramaswamy et al., 2016), and male
67 offspring from such pregnancies display similar metabolic disturbances as seen in
68 sons born to women with PCOS (Siemienowicz et al., 2019). We have reported that
69 adult prenatally androgen-excess exposed (PA) sheep have increased body weight
70 and are insulin resistant (Siemienowicz et al., 2020), while in adolescence those
71 sheep are hyperinsulinemic and have increased fat accumulation in the liver,
72 independent of body weight or central adiposity (Hogg et al., 2011). We
73 hypothesised that the metabolic phenotype of PA sheep is associated with aberrant
74 adipogenesis. Herein we investigate adipose tissue structure and function in
75 adulthood and highlight aberrant adipogenesis in adolescence and its consequences
76 in female PA sheep.

77

78 **2. Materials and Methods**

79 **2.1 Ethics statement**

80 All studies were approved by the UK Home Office and conducted under approved
81 Project Licence PPL60/4401. The Animal Research Ethics Committee of The
82 University of Edinburgh approved this study. The study was carried out in
83 accordance with the relevant guidelines.

84 **2.2 Animals and tissues**

85 Animal husbandry, experimental protocols and tissue collection were performed as
86 previously described (Hogg et al., 2012; 2011; Rae et al., 2013; Ramaswamy et al.,
87 2016). Scottish Greyface ewes were housed in groups in spacious enclosures and
88 fed hay *ad libitum*. Ewes with a healthy body condition score (2.75-3) were
89 synchronised with Chronogest (flugestone) sponges (Intervet Ltd, UK) and
90 Estrumate (cloprostenol) injection (Schering Plough Animal Health, UK) and mated
91 with Texel rams. Pregnancy was suggested by lack of estrous and confirmed by
92 ultrasound scanning.

93 In the maternal injection cohort (MI) pregnant ewes were randomised to twice weekly
94 IM 100mg testosterone propionate (TP) in 1ml vegetable oil from day (D)62 to D102
95 of D147 pregnancy or 1ml vegetable oil (control (C)).

96 In pregnancies where fetal tissue was collected (D112: C=9; PA=4), ewes were
97 sacrificed on D112 of gestation via barbiturate overdose. The gravid uterus was
98 immediately removed, fetal sex and weight recorded, and tissue of interest snap
99 frozen and stored at -80C.

100 In pregnancies carried to term, lambs were weaned at 3 months and fed hay or
101 grass *ad libitum* until sacrifice at 11 weeks [juvenile (C=8; PA=8)]; 11 months,
102 [adolescent (C=5; PA=9)] or 30 months [adult (C=11; PA=4)].

103 In the fetal injection cohort (FI), on day 62 and day 82 of gestation, mothers were
104 randomised and anaesthetised by initial sedation with 10 mg Xylazine (i.m. Rompun;
105 Bayer PLC Animal Health Division, UK), followed by 2mg/kg Ketamine (i.v, Ketaset;
106 Fort Dodge Animal Health, UK). All subsequent procedures were conducted under
107 surgical aseptic conditions. Fetuses were injected via ultrasound guidance into the
108 fetal flank with 20G Quinke spinal needle (BD Biosciences, UK) with following
109 according to the treatment group: control (C; n=12), 0.2ml vehicle (vegetable oil);
110 testosterone propionate (TP; n=7), 20mg TP in 0.2ml vehicle; diethylsilbesterol
111 (DES; n=8), 4mg DES in 0.2ml vehicle; dexamethasone (DEX; n=11), 100µg DEX in
112 0.2ml vehicle. Justification of the rationale, timing and treatment doses have been
113 published previously (Siemienowicz et al., 2019). Immediately after surgical
114 procedure completion all pregnant ewes were given prophylactic antibiotics
115 (Streptacare, Animalcare Ltd., UK, 1 ml/25 kg) and were then monitored during
116 recovery; no adverse effects of these procedures were observed. Lambs were
117 weaned at 3 months and fed hay or grass ad libitum and sacrificed in adolescence
118 (11 months of age).

119 Animals were sacrificed as described before (Hogg et al., 2011), omental tissue was
120 carefully removed and weighed, and tissues of interest were fixed in Bouins solution
121 for 24h, transferred to 70% ethanol and processed into paraffin wax and/or snap
122 frozen and stored at -80C. Visceral adipose tissue was collected from omentum and
123 subcutaneous adipose tissue from the groin area.

124 **2.3 Plasma analyte determination**

125 Concentrations of fasting plasma free fatty acids (FFAs), triglycerides (TGs), total
126 cholesterol and high-density lipoprotein (HDL) were obtained using commercial
127 assay kits (Alpha Laboratories Ltd., UK) as per manufacturer's instruction, using a

128 Cobas Mira automated analyser (Roche Diagnostics Ltd, UK). For all assays intra
129 and inter-assay CV's were < 4% CV and < 5% CV, respectively. Fasting plasma
130 leptin concentration was measured using Bio-Plex Human Diabetes Assay
131 (171A7001M; Bio-Rad, UK), as per the manufacturer's instruction. All samples were
132 assayed in duplicate and the results were acquired and calculated using Bio-Plex
133 200 array reader system with Bio-Plex Manager software (Bio-Rad, UK). The assay
134 working range for leptin was 0.011-129ng/ml, assay sensitivity 3.1pg/ml, and intra
135 and inter-assay CVs were 3% and 4%, respectively. Plasma adiponectin was
136 measured using human Adiponectin ELISA kit (KHP041; Invitrogen, Life
137 Technologies, UK), as per the manufacturer's instructions. All samples were assayed
138 in duplicate. The assay sensitivity was 0.1ng/ml intra and inter-assay CVs were <5%
139 and <6%, respectively.

140 **2.4 Adipocyte morphometric analysis**

141 For adipocyte morphometric analysis, two 5 µm sections were cut per adipose tissue
142 sample, a minimum of 100 µm apart, and mounted on positively charged slides
143 (Superfrost Plus Gold, Thermochemical, UK). Sections were then stained with
144 haematoxylin and eosin following standard protocol. Two randomly selected fields
145 per section were captured at X4 magnification using Olympus Provis BX2
146 microscope (Olympus America Inc., USA) attached to a Canon EOS 30D Microcam
147 camera (Canon Inc, Japan). Images were analysed using Adiposoft, ImageJ
148 Software (Galarraga et al., 2012) in a blinded manner. Results were then manually
149 corrected as per Adiposoft instructions and confirmed on a graticuled microscope.

150 **2.5 Western Blotting**

151 For western blotting all controls (C; n=5) and 5 samples from PA group were randomly
152 selected for the analysis. Samples were homogenised with Soniprep150 (MSE UK

153 Ltd.) in RIPA buffer (ab156034, Abcam, UK) supplemented with Halt™ Protease
154 Inhibitor Cocktail (Thermo Scientific Pierce, USA) and centrifuged at 17500g at 4°C
155 for 10 min to pellet cellular debris. Protein concentration was measured using the
156 Bradford Assay on Cobas Fara centrifugal analyser (Roche Diagnostics, UK).
157 Samples were diluted in RIPA buffer and combined with equal volume of 1X Laemmli
158 buffer (0.1M Tris-HCl pH 6.8, 20% glycerol, 2% (w/v) SDS, 0.16% (w/v) bromophenol
159 blue and 3% β-mercaptoethanol). After heat denaturation (95°C for 5 min), samples
160 (20 µg total protein) underwent electrophoresis, alongside full-range PageRuler™
161 Plus Prestained Protein Ladder (Thermo Scientific Pierce, USA), on 4-20% Tris-
162 HEPES-SDS Precast Polyacrylamide Mini Gels (Thermo Scientific Pierce, USA) and
163 were transferred to a PVDF membrane (IPFL00010; Immobilon-FL PVDF; Merck
164 Millipore, Germany) using fast semi-dry blotter (Thermo Scientific Pierce, USA).
165 Membranes were blocked in Odyssey Blocking Buffer (Li-Cor, USA) overnight at 4°C.
166 Membrane was probed with primary antibody raised against STAT1 (1:1000; SC-346,
167 Santa Cruz Biotechnology) for 2h at RT, washed and probed with a primary antibody
168 raised against PPARγ (1:500; SC-1984 Santa Cruz Biotechnology) for 4h at RT. After
169 washing, membranes were incubated with two different fluorescently-labelled
170 secondary antibodies at the concentration 1:10000 IRDye 680RD (926-68074; Li-Cor)
171 and IRDye 800CW (926-32213; Li-Cor), both for 1h at RT. After final washing,
172 membranes were visualised on the Odyssey Imager (Li-Cor, USA). The size of the
173 visualised protein band was confirmed with reference to the molecular weight markers.
174 Protein densitometry was analysed with Image Studio Lite Software (Li-Cor, USA) with
175 STAT1 protein levels used as the loading control.

176 **2.5 Quantitative (q)RT-PCR**

177 RNA was extracted from adipose tissue with a combination of TRI Reagent with the
178 RNeasy Mini Kit (Qiagen Ltd.) and from liver using RNeasy Mini Kit following the
179 manufacturer's instructions. On-column DNase digestion was performed using
180 RNase-Free DNase set (Qiagen Ltd.) and RNA concentration and purity was
181 assessed using a NanoDrop One spectrometer (ThermoFisher Scientific, UK).
182 Complimentary DNA was synthesised using TaqMan Reverse Transcription Kit
183 (Applied Biosystems, UK) as described previously (Hogg et al., 2012). To select the
184 most stable housekeeping genes the geNorm Reference Gene Selection Kit
185 (Primerdesign Ltd., UK) was used, identifying in visceral adipose tissue the suitability
186 of the geometric mean of *RPS26* and *18S*, and for subcutaneous adipose tissue and
187 liver the geometric mean of *ACTB* and *MDH1* was utilised.
188 Primers (Table 1) were designed and synthesised as described previously
189 (Siemienowicz et al., 2020). Real time RT-PCR was performed on 384-well plate
190 format (Applied Biosystems) with all samples assayed in duplicate and
191 housekeeping control genes included in each run, as well as template, RNA and RT-
192 negative controls, using the ABI 7900HT Fast Real Time PCR system (Applied
193 Biosystems) as described previously (Hogg et al., 2012). The transcript abundance
194 of target gene relative to the housekeeping genes was quantified using the $\Delta\Delta C_t$
195 method (Livak and Schmittgen, 2001).

196 **2.6 Statistical analysis**

197 All data sets were normality tested prior to further analysis (Shapiro-Wilk test), and
198 logarithmically transformed if necessary. For comparing means of two treatment
199 groups with equal variances, unpaired, two-tailed Student's t test was used
200 accepting $P < 0.05$ as significant. For more than two comparisons ANOVA was used
201 with Dunnett's post hoc test. Correlation was assessed by calculation of Pearson

202 product-moment co-efficient. Statistical analysis was performed using GraphPad
203 Prism 8.0 software (GraphPad Prism Software, San Diego, CA, USA). Asterisks
204 were used to indicate level of significance based on the following criteria: * $P < 0.05$,
205 ** $P < 0.01$.
206

207 **3. Results**

208 **3.1 PA sheep have structurally altered subcutaneous adipose tissue in** 209 **adulthood**

210 Female PA sheep prenatally programmed to develop a PCOS-like condition show no
211 difference in birth weight or body weight during the first year of life, through puberty
212 and adolescence, however, in adulthood they have increased body weight as
213 compared to controls (Siemienowicz et al., 2020). Adipocyte morphology was
214 assessed by histological morphometric analysis (Fig. 1A). In VAT there was no
215 difference in the numbers of adipocytes per mm² (Fig. 1B), no change in the mean
216 size of adipocytes (Fig. 1C) and no alteration the number of adipocytes of different
217 sizes (Fig. 1D). In contrast, adipocyte number was decreased in SAT (Fig. 1E;
218 $P<0.05$), with a trend to an augmented mean size of adipocytes (Fig. 1F; $P=0.06$) as
219 a result of an increased number of large adipocytes (defined as larger than 5000
220 μm^2) (Fig. 1G; $P<0.05$). The increased number of large SAT adipocytes in PA sheep
221 was not a consequence of increased body weight as the difference was also
222 observed between a weight-matched subset of controls ($n=4$) and PA sheep ($n=4$)
223 (Fig. 1H; $P<0.05$). Key transcriptional regulators of adipogenesis, *PPARG*, *CEBPA*,
224 *CEBPB* and *CEBPD* were not altered in adult VAT or SAT (Fig. 1I). There are fewer,
225 but larger adipocytes in SAT in PA sheep but this was not associated with alterations
226 in adipogenesis in adulthood.

227 **3.2 Prenatal androgen excess is associated with adipose tissue dysfunction in** 228 **adulthood**

229 There were no differences in the transcript abundance of markers of mature
230 adipocytes (*LEP* and *ADIPOQ*) in VAT or SAT (Fig. 2A) in adult PA sheep.
231 Furthermore, there was no difference in plasma concentrations (Fig. 2B,C), although

232 there was a trend towards decreased adiponectin level (Fig. 2C; P=0.08) in PA
233 sheep when compared to controls. There were no differences in transcript
234 abundance of inflammatory markers in VAT (Fig. 2D) while in SAT PA sheep had
235 increased *TNF* (P<0.05), *IL6* (P<0.05) and *CCL2* (P<0.05) when compared to
236 controls (Fig. 2E; P<0.05). Although the PA sheep have normal levels of TGs,
237 cholesterol and HDL cholesterol (Fig. 3A-C) they have increased circulating FFAs
238 (Fig. 3D; P<0.05). There was negative correlation (r= -0.66) between the total
239 number of adipocytes per mm² and the levels of circulating FFAs (Fig. 3E; P<0.05).
240 Although at this time there was no difference in omental fat (Fig. 3F) there was
241 increased transcript abundance of genes involved in fat uptake and accumulation in
242 VAT (*SLC27A1*, *CAV1*, *CAV2*, *FABP5* and *LPIN2*) (Fig. 3G-K; P<0.05). Alterations in
243 adipose tissue associated with inflammation is seen in SAT only and this is
244 associated with increased FFAs. In summary, we observed structurally altered
245 subcutaneous adipose tissue, with attendant dysfunction in adulthood attributable to
246 prenatal androgen excess.

247 **3.3 Altered adipogenesis is observed during adolescence**

248 We next assessed expression of transcription factors involved in adipogenesis at 11
249 months of age when there was no difference in body weight (Siemienowicz et al.,
250 2020) and omental fat weight (Hogg et al., 2011). In VAT there was no difference in
251 the transcript abundance of *PPARG*, *CEBPA* and *CEBPB*, although *CEBPD* was
252 increased (P<0.05) in adolescent PA sheep (Fig. 4A). However, in SAT there was
253 decreased transcript abundance of *PPARG*, *CEBPA*, *CEBPB* (Fig. 4B; P<0.05) but
254 no difference in *CEBPD* (Fig. 4B). We confirmed decreased level of *PPARG* in SAT
255 (Fig. 4C; P<0.05) in adolescent PA females, by Western blot. In addition, adolescent
256 PA sheep had decreased expression of markers of mature adipocytes in SAT,

257 *SLC2A4* and *PLIN1* (Supplementary Figure 1; $P < 0.05-0.01$). In order to determine
258 the specificity of prenatal androgens in the regulation of adolescent adipogenesis
259 (Fig. 4D) we directly injected various steroids into the mid-gestation fetus and
260 assessed adipogenesis markers in SAT in adolescence. Reduced adipogenesis-
261 associated gene expression in SAT was only associated with prenatal androgen
262 excess (TP) and neither estrogenic (DES) excess nor glucocorticoid (DEX) excess
263 showed similar effects (Fig. 4D; $P < 0.05$).

264 **3.4 Adolescent SAT transcriptional alterations are associated with increased** 265 **circulating FFA**

266 Fasting FFAs were increased in adolescent PA sheep when compared to controls
267 (Fig. 5A; $P < 0.05$). Their concentrations were negatively correlated with *PPARG* ($r = -$
268 0.55) in SAT (Fig. 5B; $P < 0.05$) but not with *PPARG* in VAT (Fig. 5C). These sheep
269 have early accumulation of fat in the liver (Hogg et al., 2011) with increased
270 transcript abundance of genes involved in FFAs uptake and deposition in the liver
271 (Fig. 5D-F; $P < 0.05$).

272 **3.5 Adiponectin is a biomarker of reduced SAT adipogenesis during** 273 **adolescence**

274 To investigate potential biomarkers of altered adipogenesis during adolescence the
275 transcript abundance of markers of mature adipocytes was investigated in adipose
276 tissue at 11 months of age in control and PA animals. In VAT there was no changes
277 in *LEP* or *ADIPOQ* expression (Fig. 6A,B). In contrast *LEP* ($P < 0.01$) and *ADIPOQ*
278 ($P < 0.05$) were reduced in SAT in adolescent PA sheep when compared to controls
279 (Fig. 6C,D). This was reflected by a reduction in circulating leptin (Fig 6E; $P < 0.05$)
280 and adiponectin (Fig. 6F; $P < 0.05$) in the plasma. Circulating adiponectin correlated
281 ($r = 0.79$) to *ADIPOQ* in SAT (Fig. 6G; $P < 0.01$) but not VAT (Fig. 6H), and there was

282 no correlation identified between circulating leptin and SAT *LEP* gene expression.

283 Collectively, in female PA offspring, we observed altered adipogenesis during
284 adolescence, with increased circulating FFA, and this response was specific to
285 androgenic excess during development. Reduced circulating adiponectin has
286 potential as a biomarker of reduced adipogenesis in SAT during adolescence.

287 **3.6 *There is no evidence of altered adipogenesis before puberty***

288 Altered transcript abundance for transcription factors involved in adipogenesis was
289 not observed pre-pubertally at 11 weeks of age or in fetal life (Table 1).

290

291 **4. Discussion**

292 We demonstrated, using an ovine model of PCOS, that during adolescence, but not
293 fetal or prepubertal life, there was decreased adipogenesis in SAT in PA sheep. This
294 was accompanied by decreased concentrations of leptin and adiponectin, and
295 increased concentrations of FFAs, likely underpinning the observation of upregulated
296 expression of FFAs transporters in liver. Adult consequences of such altered
297 adolescent adipogenesis were that PA female offspring displayed adipocyte
298 hypertrophy in SAT paralleled by increased expression of inflammatory markers and
299 increased expression of genes linked to fat accumulation in VAT.

300

301 In fetal life pre-adipocyte differentiation into adipocytes occurs between the 14th and
302 the 16th weeks of gestation in humans (Poissonnet et al., 1983) and in the third
303 month of gestation in sheep (Wensvoort, 1967). In late gestation adipocyte
304 proliferation decreases, and until adolescence, increased adiposity primarily occurs
305 via filling of predetermined adipocytes. During puberty another window of adipocyte
306 proliferation occurs (Rosen and Spiegelman, 2014) setting the total number of
307 adipocytes. Whilst differentiation potential of pre-adipocytes into mature adipocytes
308 is present throughout life, dependent upon energy status and storage needs (Rosen
309 and Spiegelman, 2014), in adult life, the capacity of preadipocytes to become fully
310 functional mature adipocytes declines (Tchkonina et al., 2010). Hence increased or
311 decreased adult body weight, with corresponding fluctuations in body fat mass, is
312 reflective of changes in adipocyte volume but not number (MacLean et al., 2015;
313 Spalding et al., 2008). In our study altered adipogenesis in SAT of PA females was
314 only evident during adolescence (11 months).

315

316 During adipogenesis, pre-adipocyte terminal differentiation to mature adipocytes
317 involves accruing lipid transport and synthesis capacity, insulin responsiveness and
318 synthesis of adipokines, regulated by PPARG and the family of CCAAT/enhancer
319 binding protein transcription factors (C/EBP) (Cristancho and Lazar, 2011). SAT
320 expansion improves lipid buffering and metabolic profile (Kim et al., 2007) while
321 inability to increase adipose cell number results in hypertrophic adipocytes,
322 increasing risk of metabolic diseases (Dubois et al., 2006). Impaired SAT
323 adipogenesis results in decreased storage capacity, and accumulation of lipids in
324 non-adipose tissues, lipotoxicity and metabolic perturbations (Carobbio et al., 2017).
325 Furthermore, decreased subcutaneous pre-adipocyte differentiation and defective
326 storage capacity of SAT are associated with increased visceral adiposity (Alligier et
327 al., 2013; Lessard et al., 2014), suggesting increased visceral fat accumulation might
328 be a compensatory adaptation to limitations in SAT expandability (Britton and Fox,
329 2011).

330

331 Decreased expression of PPARG, *CEBPA* and *CEBPB* in SAT, in PA sheep
332 suggests decreased differentiation of pre-adipocytes into mature adipocytes and
333 indicates lower capacity of SAT to safely store fat, which combined with observations
334 of increased levels of FFAs in PA adolescent sheep supports suggestions of
335 decreased lipid storage volume in SAT. This may also contribute to fatty liver
336 development due to increased release of FFAs into circulation and increased hepatic
337 uptake (Hogg et al., 2011). Morphometric analysis of the SAT in adolescent sheep
338 was not performed due to lack of histological samples, as the aim of the study was to
339 determine adult outcomes in terms of adipose structure, and examine the earlier life
340 mechanistic antecedents of any altered adult structure observed; we acknowledge

341 this limitation of the data presented here. Veiga-Lopez *et al.* previously reported that
342 postpubertal, (21 months old), prenatally androgenised female sheep showed
343 reduction in adipocyte cell size in both VAT and SAT and concluded failure of a
344 subset of small adipocytes to differentiate. (Veiga-Lopez *et al.*, 2013). We did not
345 observe any effect on VAT in our adolescent animals. The discrepancies between
346 studies may be attributed to different timing of the prenatal testosterone treatment
347 and different age at study.

348 Adipogenesis in PCOS patients has not been thoroughly investigated, however,
349 increased abdominal adipose stem cell commitment to preadipocytes *in vitro*, as
350 measured by the expression of ZFP423 protein, have been found in adult, normal
351 weight women with PCOS (Fisch *et al.*, 2018). Increased *ZFP423* gene expression
352 was also reported in abdominal SAT of prenatally androgenised female rhesus
353 monkeys (Keller *et al.*, 2014). We did not study the preadipocyte commitment but
354 rather, the differentiation of preadipocytes into mature adipocytes. In agreement with
355 our study, it was reported that women with PCOS have decreased expression and
356 increased DNA methylation of *PPARG* in SAT and *PPARG* expression positively
357 correlated with insulin sensitivity and negatively with adipocyte size and testosterone
358 levels (Kokosar *et al.*, 2016). Furthermore, PCOS-like monkeys were also have
359 decreased abdominal SAT *CEBPA* expression, reduced numbers of mature SAT
360 adipocytes and increased FFAs indicating impaired adipogenesis (Keller *et al.*,
361 2014). In addition, there is growing evidence of decreased adipogenesis in SAT from
362 insulin resistant individuals and subjects with abdominal obesity (Heilbronn *et al.*,
363 2004; Permana *et al.*, 2004; Yang *et al.*, 2004). Our data is in broad agreement with
364 such observations, lending translational confidence to our findings.

365

366 Further translational relevance in terms of PCOS is derived from observations that
367 obese adolescent girls with PCOS have persistently elevated FFAs when compared
368 with obese controls (King et al., 2017). Since SAT represents approximately 80% of
369 total body adipose tissue, decreased SAT adipogenesis in adolescence may
370 predispose to decreased storage capacity in adulthood and increased adipocyte
371 hypertrophy. In support of this, our adult PA sheep have decreased SAT adipocyte
372 numbers and corresponding increased numbers of large, hypertrophic adipocytes,
373 and adult PCOS women have hypertrophic adipocytes in SAT (Echiburú et al., 2018;
374 Faulds et al., 2003; Manneras-Holm et al., 2010).

375

376 Hypertrophic expansion of SAT is associated with altered adipokine secretion,
377 inflammation and fibrosis (Longo et al., 2019). Adipocyte hypertrophy in adult PA
378 sheep was paralleled by increased expression of *TNF*, *IL6* and *CCL2* in SAT.
379 Enlarged adipocytes overexpress MCP-1 (encoded by *CCL2* gene) and induce
380 increased recruitment of proinflammatory M1 macrophages culminating in increased
381 production of pro-inflammatory cytokines $TNF\alpha$ and IL-6, promoting altered gene
382 expression and insulin resistance in adipocytes (Weisberg et al., 2003).

383

384 Adolescent PA sheep had also decreased expression of markers of mature
385 adipocytes *LEP* and *ADIPOQ* in SAT, functionally realised by decreased circulating
386 leptin and adiponectin concentrations. There was positive correlation of *ADIPOQ*
387 mRNA in SAT, with circulating adiponectin, reminiscent of that observed in women
388 with PCOS (Echiburú et al., 2018; Lecke et al., 2013), and suggesting the likelihood
389 that decreased adiponectin levels in adolescent PCOS-like sheep is a consequence
390 of decreased adipogenesis in SAT. Adiponectin, primarily secreted from SAT, is an

391 insulin sensitising adipokine, promoting lipid oxidation and reducing plasma
392 concentration of FFAs (Achari and Jain, 2017), and stimulates glucose uptake in
393 adipocytes by increasing expression of GLUT4 (Achari and Jain, 2017; Fu et al.,
394 2005).

395

396 Adiponectin is also an autocrine factor promoting and regulating adipocyte
397 differentiation (do Carmo Avides et al., 2008; Fu et al., 2005). Decreased circulating
398 adiponectin levels, independent of adiposity, are consistently reported in adolescent
399 and adult PCOS patients (Cankaya et al., 2014; Escobar-Morreale et al., 2006;
400 Maliqueo et al., 2012; Mirza et al., 2014; Sepilian and Nagamani, 2005), suggesting
401 potential utility as a biomarker of PCOS (Al-Awadi et al., 2016; Sarray et al., 2015).

402 Whilst androgens decrease plasma adiponectin *in vitro* and *in vivo* (Frederiksen et
403 al., 2012; Nishizawa et al., 2002; Xu et al., 2005), and this is inversely correlated with
404 testosterone levels, (Böttner et al., 2004; Riestra et al., 2013), to our knowledge this
405 is the first demonstration of prenatal androgen excess being associated with
406 decreased SAT and circulating adiponectin. It is noteworthy in the context of prenatal
407 androgenic programming of PCOS that adiponectin decreases ovarian thecal
408 androgen synthesis and expression of adiponectin receptors is decreased in theca
409 cells from polycystic ovaries; consequently decreased adiponectin may also
410 contribute to hyperandrogenism in PCOS women (Comim et al., 2013; Lagaly et al.,
411 2008).

412

413 Inhibitory effects of androgens on adipogenesis is well documented (Zerradi et al.,
414 2014). Numerous studies demonstrate androgens prevent *in vitro* differentiation and
415 proliferation of murine preadipocyte cell lines (Fujioka et al., 2012; Singh et al., 2003;

416 2005) and human preadipocytes from both sexes, and from different fat depots
417 (Blouin et al., 2010; Chazenbalk et al., 2013; Gupta et al., 2008; McNelis et al.,
418 2013). To determine steroid specificity of androgenic excess in programming
419 adipose tissue function *in vivo*, we assessed SAT adipogenesis in adolescent, 11
420 months old female sheep, that were directly injected *in utero* with androgen,
421 estrogen (DES as surrogate estrogen) or glucocorticoid (DEX as surrogate, active
422 glucocorticoid). We found that only androgen treatment, but not estrogen or
423 glucocorticoid, decreased adipogenesis in SAT in adolescence, identifying that the
424 responses measured throughout the study were androgenic.

425

426 In summary, we have shown that during adolescence, altered adipogenesis in SAT
427 of PA sheep occurs, with decreased beneficial adipokines, independent of central
428 adiposity. Decreased adipocyte differentiation during adolescence resulted in
429 hypertrophy and inflammation of adult SAT. This decreased capacity of SAT to
430 safely store fat may explain metabolic perturbations observed in PA female sheep,
431 shedding light upon new investigatory, and interventional avenues in clinical PCOS
432 research.

433

434 **Acknowledgements**

435 The authors wish to acknowledge Joan Docherty, John Hogg, Marjorie Thomson,
436 Peter Tennant and James Nixon and the staff at the Marshall Building, University of
437 Edinburgh for their excellent animal husbandry. Dr Kirsten Hogg, Dr Fiona Connolly,
438 Dr Junko Nio-Kobayashi, Dr Avi Lerner and Lyndsey Boswell helped with tissue
439 collection.

440

441 **Funding**

442 This work was funded by Medical Research Council (MRC) project grants
443 (G0500717; G0801807; G0802782; MR/P011535/1) and supported by the MRC
444 Centre for Reproductive Health (MR/N022556/1).

445

446 **Declaration of interest**

447 The authors have no conflicts of interest to declare.

448

449 **References**

- 450 Abbott, D.H., Nicol, L.E., Levine, J.E., Xu, N., Goodarzi, M.O., Dumesic, D.A., 2013.
451 Nonhuman primate models of polycystic ovary syndrome. *Mol. Cell. Endocrinol.* 373,
452 21–28. doi:10.1016/j.mce.2013.01.013
453
- 454 Achari, A.E., Jain, S.K., 2017. Adiponectin, a Therapeutic Target for Obesity,
455 Diabetes, and Endothelial Dysfunction. *Int. J. Mol. Sci.* 18, 1321.
456 doi:10.3390/ijms18061321
457
- 458 Al-Awadi, A.M., Sarray, S., Arekat, M.R., Saleh, L.R., Mahmood, N., Almawi, W.Y.,
459 2016. The high-molecular weight multimer form of adiponectin is a useful marker of
460 polycystic ovary syndrome in Bahraini Arab women. *Clin. Nutr. ESPEN* 13, e33–e38.
461 doi:10.1016/j.clnesp.2016.03.078
462
- 463 Alligier, M., Gabert, L., Meugnier, E., Lambert-Porcheron, S., Chanseaume, E.,
464 Pilleul, F., Debard, C., Sauvinet, V., Morio, B., Vidal-Puig, A., Vidal, H., Laville, M.,
465 2013. Visceral fat accumulation during lipid overfeeding is related to subcutaneous
466 adipose tissue characteristics in healthy men. *J. Clin. Endocrinol. Metab.* 98, 802–
467 810. doi:10.1210/jc.2012-3289
468
- 469 Blouin, K., Nadeau, M., Perreault, M., Veilleux, A., Drolet, R., Marceau, P., Mailloux,
470 J., Luu-The, V., Tchernof, A., 2010. Effects of androgens on adipocyte differentiation
471 and adipose tissue explant metabolism in men and women. *Clin. Endocrinol.* 72,
472 176–188. doi:10.1111/j.1365-2265.2009.03645.x

473 Böttner, A., Kratzsch, J., Müller, G., Kapellen, T.M., Blüher, S., Keller, E., Blüher, M.,
474 Kiess, W., 2004. Gender Differences of Adiponectin Levels Develop during the
475 Progression of Puberty and Are Related to Serum Androgen Levels. *J. Clin.*
476 *Endocrinol. Metab.* 89, 4053–4061. doi:10.1210/jc.2004-0303
477
478 Britton, K.A., Fox, C.S., 2011. Ectopic Fat Depots and Cardiovascular Disease.
479 *Circulation* 124, e837-41. doi:10.1161/CIRCULATIONAHA.111.077602
480
481 Cankaya, S., Demir, B., Aksakal, S.E., Dilbaz, B., Demirtas, C., Goktolga, U., 2014.
482 Insulin resistance and its relationship with high molecule weight adiponectin in
483 adolescents with polycystic ovary syndrome and a maternal history. *Fertil. Steril.*
484 102, 826–830. doi:10.1016/j.fertnstert.2014.05.032
485
486 Carmina, E., Orio, F., Palomba, S., Cascella, T., Longo, R.A., Colao, A.M.,
487 Lombardi, G., Lobo, R.A., 2005. Evidence for altered adipocyte function in polycystic
488 ovary syndrome. *Eur. J. Endocrinol.* 152, 389–394. doi:10.1530/eje.1.01868
489
490 Carobbio, S., Pellegrinelli, V., Vidal-Puig, A., 2017. Adipose Tissue Function and
491 Expandability as Determinants of Lipotoxicity and the Metabolic Syndrome. *Adv.*
492 *Exp. Med. Biol.* 960, 161–196. doi:10.1007/978-3-319-48382-5_7
493
494 Chazenbalk, G., Singh, P., Irge, D., Shah, A., Abbott, D.H., Dumesic, D.A., 2013.
495 Androgens inhibit adipogenesis during human adipose stem cell commitment to
496 preadipocyte formation. *Steroids* 78, 920–926. doi:10.1016/j.steroids.2013.05.001

497 Comim, F.V., Hardy, K., Franks, S., 2013. Adiponectin and Its Receptors in the
498 Ovary: Further Evidence for a Link between Obesity and Hyperandrogenism in
499 Polycystic Ovary Syndrome. PLoS ONE 8, e80416.
500 doi:10.1371/journal.pone.0080416
501
502 Cristancho, A.G., Lazar, M.A., 2011. Forming functional fat: a growing understanding
503 of adipocyte differentiation. Nat. Rev. Mol. Cell Biol. 12, 722–734.
504 doi:10.1038/nrm3198
505
506 do Carmo Avides, M., Domingues, L., Vicente, A., Teixeira, J., 2008. Differentiation
507 of human pre-adipocytes by recombinant adiponectin. Protein Expr. Purif. 59, 122–
508 126. doi:10.1016/j.pep.2008.01.012
509
510 Dubois, S.G., Heilbronn, L.K., Smith, S.R., Albu, J.B., Kelley, D.E., Ravussin, E.,
511 Look AHEAD Adipose Research Group, 2006. Decreased expression of adipogenic
512 genes in obese subjects with type 2 diabetes. Obesity 14, 1543–1552.
513 doi:10.1038/oby.2006.178
514
515 Echiburú, B., Pérez-Bravo, F., Galgani, J.E., Sandoval, D., Saldías, C., Crisosto, N.,
516 Maliqueo, M., Sir-Petermann, T., 2018. Enlarged adipocytes in subcutaneous
517 adipose tissue associated to hyperandrogenism and visceral adipose tissue volume
518 in women with polycystic ovary syndrome. Steroids 130, 15–21.
519 doi:10.1016/j.steroids.2017.12.009
520

521 Escobar-Morreale, H.F., Villuendas, G., Botella-Carretero, J.I., Álvarez-Blasco, F.,
522 Sanchón, R., Luque-Ramírez, M., Millán, J.L.S., 2006. Adiponectin and resistin in
523 PCOS: a clinical, biochemical and molecular genetic study. *Hum. Reprod.* 21, 2257–
524 2265. doi:10.1093/humrep/del146

525

526 Faulds, G., Ryden, M., Ek, I., 2003. Mechanisms behind lipolytic catecholamine
527 resistance of subcutaneous fat cells in the polycystic ovarian syndrome. *J. Clin.*
528 *Endocrinol. Metab.* 88, 2269. doi:10.1210/jc.2002-021573

529

530 Fauser BCJM, Tarlatzis BC, Rebar RW, Legro RS, Balen AH, Lobo R, Carmina E,
531 Chang J, Yildiz BO, Laven JSE *et al.* 2012 Consensus on women's health aspects of
532 polycystic ovary syndrome (PCOS): the Amsterdam ESHRE/ASRM-Sponsored 3rd
533 PCOS Consensus Workshop Group. *Hum. Reprod.* 27, 14-24. doi:
534 10.1093/humrep/der396

535

536 Fisch, S.C., Nikou, A.F., Wright, E.A., Phan, J.D., Leung, K.L., Grogan, T.R., Abbott,
537 D.H., Chazenbalk, G.D., Dumesic, D.A., 2018. Precocious subcutaneous abdominal
538 stem cell development to adipocytes in normal-weight women with polycystic ovary
539 syndrome. *Fertil. Steril.* 110, 1367–1376. doi:10.1016/j.fertnstert.2018.08.042

540

541 Frederiksen, L., Højlund, K., Hougaard, D.M., Mosbech, T.H., Larsen, R., Flyvbjerg,
542 A., Frystyk, J., Brixen, K., Andersen, M., 2012. Testosterone therapy decreases
543 subcutaneous fat and adiponectin in aging men. *Eur. J. Endocrinol.* 166, 469–476.
544 doi:10.1530/EJE-11-0565

545

546 Fu, Y., Luo, N., Klein, R.L., Garvey, W.T., 2005. Adiponectin promotes adipocyte
547 differentiation, insulin sensitivity, and lipid accumulation. *J. Lipid Res.* 46, 1369–
548 1379. doi:10.1194/jlr.M400373-JLR200
549

550 Fujioka, K., Fujioka, K., Kajita, K., Kajita, K., WU, Z., Hanamoto, T., Wu, Z.,
551 Hanamoto, T., Ikeda, T., Ikeda, T., Mori, I., Okada, H., Mori, I., Okada, H., Yamauchi,
552 M., Yamauchi, M., Uno, Y., Morita, H., Uno, Y., Nagano, I., Morita, H., Takahashi, Y.,
553 Nagano, I., Takahashi, Y., Ishizuka, T., Ishizuka, T., 2012. Dehydroepiandrosterone
554 reduces preadipocyte proliferation via androgen receptor. *Am. J. Physiol. Endocrinol.*
555 *Metab.* 302, E694–704. doi:10.1152/ajpendo.00112.2011
556

557 Galarraga, M., Campión, J., Muñoz-Barrutia, A., Boqué, N., Moreno, H., Martínez,
558 J.A., Milagro, F., Ortiz-de-Solórzano, C., 2012. Adiposoft: automated software for the
559 analysis of white adipose tissue cellularity in histological sections. *J. Lipid Res.* 53,
560 2791–2796. doi:10.1194/jlr.D023788
561

562 Gupta, V., Bhasin, S., Guo, W., Singh, R., Miki, R., Chauhan, P., Choong, K.,
563 Tchkonina, T., Lebrasseur, N.K., Flanagan, J.N., Hamilton, J.A., Viereck, J.C., Narula,
564 N.S., Kirkland, J.L., Jasuja, R., 2008. Effects of dihydrotestosterone on differentiation
565 and proliferation of human mesenchymal stem cells and preadipocytes. *Mol. Cell.*
566 *Endocrinol.* 296, 32–40. doi:10.1016/j.mce.2008.08.019
567

568 Heilbronn, L., Smith, S.R., Ravussin, E., 2004. Failure of fat cell proliferation,
569 mitochondrial function and fat oxidation results in ectopic fat storage, insulin

570 resistance and type II diabetes mellitus. *Int. J. Obes.* 28, S12–S21.
571 doi:10.1038/sj.ijo.0802853
572
573 Hogg, K., Wood, C., McNeilly, A.S., Duncan, W.C., 2011. The in utero programming
574 effect of increased maternal androgens and a direct fetal intervention on liver and
575 metabolic function in adult sheep. *PLoS ONE* 6, e24877.
576 doi:10.1371/journal.pone.0024877
577
578 Hogg, K., Young, J.M., Oliver, E.M., Souza, C.J., McNeilly, A.S., Duncan, W.C.,
579 2012. Enhanced Thecal Androgen Production Is Prenatally Programmed in an Ovine
580 Model of Polycystic Ovary Syndrome. *Endocrinology* 153, 450–461.
581 doi:10.1210/en.2011-1607
582
583 Jason, J., 2011. Polycystic ovary syndrome in the United States: clinical visit rates,
584 characteristics, and associated health care costs. *Arch. Intern. Med.* 171, 1209–
585 1211. doi:10.1001/archinternmed.2011.288
586
587 Keller, E., Chazenbalk, G.D., Aguilera, P., Madrigal, V., Elashoff, D., Grogan, T.,
588 Dumesic, D.A., Abbott, D.H., 2014. Impaired preadipocyte differentiation into
589 adipocytes in subcutaneous abdominal adipose of PCOS-like female rhesus
590 monkeys. *Endocrinology* 155, 2696–2703. doi:10.1210/en.2014-1050
591
592 Kim, J.-Y., van de Wall, E., Laplante, M., Azzara, A., Trujillo, M.E., Hofmann, S.M.,
593 Schraw, T., Durand, J.L., Li, H., Li, G., Jelicks, L.A., Mehler, M.F., Hui, D.Y.,
594 Deshaies, Y., Shulman, G.I., Schwartz, G.J., Scherer, P.E., 2007. Obesity-

595 associated improvements in metabolic profile through expansion of adipose tissue. J.
596 Clin. Invest. 117, 2621–2637. doi:10.1172/JCI31021
597
598 King, M., Dorosz, J., Patel, S.S., Kinney, G.L., Cree-Green, M., Wang, H., Ferland,
599 A., Truong, U., Nadeau, K.J., Maahs, D.M., Eckel, R.H., Moreau, K.L., Hokanson,
600 J.E., 2017. Obese adolescents with polycystic ovarian syndrome have elevated
601 cardiovascular disease risk markers. Vasc. Med. 22, 85–95.
602 doi:10.1177/1358863X16682107
603
604 Klemm, D.J., Leitner, J.W., Watson, P., Nesterova, A., Reusch, J., Goalstone, M.L.,
605 Draznin, B., 2001. Insulin-induced adipocyte differentiation - Activation of CREB
606 rescues adipogenesis from the arrest caused by inhibition of prenylation. J. Biol.
607 Chem. 276, 28430–28435. doi:10.1074/jbc.m103382200
608
609 Kokosar, M., Benrick, A., Perfilyev, A., Fornes, R., Nilsson, E., Maliqueo, M., Behre,
610 C.J., Sazonova, A., Ohlsson, C., Ling, C., Stener-Victorin, E., 2016. Epigenetic and
611 Transcriptional Alterations in Human Adipose Tissue of Polycystic Ovary Syndrome
612 SCI. Rep. 6, 22883. doi:10.1038/srep22883
613
614 Lafontan, M., 2014. Adipose tissue and adipocyte dysregulation. Diabetes Metab.
615 40, 16–28. doi:10.1016/j.diabet.2013.08.002
616
617 Lagaly, D.V., Aad, P.Y., Grado-Ahuir, J.A., Hulsey, L.B., Spicer, L.J., 2008. Role of
618 adiponectin in regulating ovarian theca and granulosa cell function. Mol. Cell.
619 Endocrinol. 284, 38–45. doi:10.1016/j.mce.2008.01.007

620 Lecke, S.B., Morsch, D.M., Spritzer, P.M., 2013. Association between adipose tissue
621 expression and serum levels of leptin and adiponectin in women with polycystic
622 ovary syndrome. *Genet. Mol. Res.* 12, 4292–4296. doi:10.4238/2013.February.28.16
623

624 Lessard, J., Laforest, S., Pelletier, M., Leboeuf, M., Blackburn, L., Tchernof, A.,
625 2014. Low abdominal subcutaneous preadipocyte adipogenesis is associated with
626 visceral obesity, visceral adipocyte hypertrophy, and a dysmetabolic state. *Adipocyte*
627 3, 197–205. doi:10.4161/adip.29385
628

629 Livak, K.J., Schmittgen, T.D., 2001. Analysis of Relative Gene Expression Data
630 Using Real-Time Quantitative PCR and the $2^{-\Delta\Delta CT}$ Method. *Methods* 25, 402–408.
631 doi:10.1006/meth.2001.1262
632

633 Longo, M., Zatterale, F., Naderi, J., Parrillo, L., Formisano, P., Raciti, G.A., Beguinot,
634 F., Miele, C., 2019. Adipose Tissue Dysfunction as Determinant of Obesity-
635 Associated Metabolic Complications. *Int. J. Mol. Sci.* 20, 2358.
636 doi:10.3390/ijms20092358
637

638 MacLean, P.S., Higgins, J.A., Giles, E.D., Sherk, V.D., Jackman, M.R., 2015. The
639 role for adipose tissue in weight regain after weight loss. *Obes. Rev.* 16, 45–54.
640 doi:10.1111/obr.12255
641

642 Macotela, Y., Emanuelli, B., Mori, M.A., Gesta, S., 2012. Intrinsic differences in
643 adipocyte precursor cells from different white fat depots. *Diabetes* 61, 1691–1699.
644 doi:10.2337/db11-1753

645

646 Maliqueo, M., Maliqueo, M., Pérez-Bravo, F., Galgani, J.E., Galgani, J.E., Pérez, F.,
647 Echiburú, B., Echiburú, B., Crisosto, N., de Guevara, A.L., Sir-Petermann, T., 2012.
648 Relationship of serum adipocyte-derived proteins with insulin sensitivity and
649 reproductive features in pre-pubertal and pubertal daughters of polycystic ovary
650 syndrome women. *Eur. J. Obstet. Gynecol. Reprod. Biol.* 161, 56–61.
651 doi:10.1016/j.ejogrb.2011.12.012

652

653 Manneras-Holm, L., Leonhardt, H., Jennische, E., Kullberg, J., Oden, A., Holm, G.,
654 Hellstrom, M., Lonn, L., Olivecrona, G., Stener-Victorin, E., Lonn, M., 2010. Adipose
655 tissue has aberrant morphology and function in PCOS: enlarged adipocytes and low
656 serum adiponectin, but not circulating sex steroids, are strongly associated with
657 insulin resistance. *J. Clin. Endocrinol. Metab.* 96, E304–11. doi:10.1210/jc.2010-
658 1290

659

660 McNelis, J.C., Manolopoulos, K.N., Gathercole, L.L., Bujalska, I.J., Stewart, P.M.,
661 Tomlinson, J.W., Arlt, W., 2013. Dehydroepiandrosterone exerts antiglucocorticoid
662 action on human preadipocyte proliferation, differentiation, and glucose uptake. *Am.*
663 *J. Physiol. Endocrinol. Metab.* 305, E1134–44. doi:10.1152/ajpendo.00314.2012

664

665 Mirza, S.S., Shafique, K., Shaikh, A.R., Khan, N.A., Anwar Qureshi, M., Qureshi,
666 M.A., 2014. Association between circulating adiponectin levels and polycystic
667 ovarian syndrome. *J. Ovarian Res.* 7, 18. doi:10.1186/1757-2215-7-18

668 Moran, L.J., Teede, H.J., Norman, R.J., 2015. Metabolic risk in PCOS: phenotype
669 and adiposity impact. *Trends Endocrinol. Metab.* 26, 136–143.
670 doi:10.1016/j.tem.2014.12.003
671

672 Nishizawa, H., Shimomura, I., Kishida, K., Maeda, N., Kuriyama, H., Nagaretani, H.,
673 Matsuda, M., Kondo, H., Furuyama, N., Kihara, S., Nakamura, T., Tochino, Y.,
674 Funahashi, T., Matsuzawa, Y., 2002. Androgens decrease plasma adiponectin, an
675 insulin-sensitizing adipocyte-derived protein. *Diabetes* 51, 2734–2741.
676

677 Padmanabhan, V., Veiga-Lopez, A., 2013. Sheep models of polycystic ovary
678 syndrome phenotype. *Mol. Cell. Endocrinol.* 373, 8–20.
679 doi:10.1016/j.mce.2012.10.005
680

681 Permana, P.A., Nair, S., Lee, Y.-H., Luczy-Bachman, G., Vozarova De Courten, B.,
682 Tataranni, P.A., 2004. Subcutaneous abdominal preadipocyte differentiation in vitro
683 inversely correlates with central obesity. *Am. J. Physiol. Endocrinol. Metab.* 286,
684 E958–62. doi:10.1152/ajpendo.00544.2003
685

686 Poissonnet, C.M., Burdi, A.R., Bookstein, F.L., 1983. Growth and development of
687 human adipose tissue during early gestation. *Early Hum. Dev.* 8, 1–11.
688 doi:10.1016/0378-3782(83)90028-2
689

690 Puder, J.J., Varga, S., Kraenzlin, M., De Geyter, C., Keller, U., Müller, B., 2005.
691 Central fat excess in polycystic ovary syndrome: relation to low-grade inflammation

692 and insulin resistance. *J. Clin. Endocrinol. Metab.* 90, 6014–6021.
693 doi:10.1210/jc.2005-1002
694
695 Puttabyatappa, M., Lu, C., Martin, J.D., Chazenbalk, G., Dumesic, D.,
696 Padmanabhan, V., 2018. Developmental Programming: Impact of Prenatal
697 Testosterone Excess on Steroidal Machinery and Cell Differentiation Markers in
698 Visceral Adipocytes of Female Sheep. *Reprod. Sci.* 25, 1010–1023.
699 doi:10.1177/1933719117746767
700
701 Rae, M., Grace, C., Hogg, K., Wilson, L.M., McHaffie, S.L., Ramaswamy, S.,
702 MacCallum, J., Connolly, F., McNeilly, A.S., Duncan, C., 2013. The pancreas is
703 altered by in utero androgen exposure: implications for clinical conditions such as
704 polycystic ovary syndrome (PCOS). *PLoS ONE* 8, e56263.
705 doi:10.1371/journal.pone.0056263
706
707 Ramaswamy, S., Grace, C., Mattei, A.A., Siemienowicz, K., Brownlee, W.,
708 MacCallum, J., McNeilly, A.S., Duncan, W.C., Rae, M.T., 2016. Developmental
709 programming of polycystic ovary syndrome (PCOS): prenatal androgens establish
710 pancreatic islet α/β cell ratio and subsequent insulin secretion. *Sci. Rep.* 6, 27408.
711 doi:10.1038/srep27408
712
713 Riestra, P., Garcia-Anguila, A., Ortega, L., Garces, C., 2013. Relationship of
714 Adiponectin with Sex Hormone Levels in Adolescents. *Horm. Res. Paediatr.* 79, 83–
715 87. doi:10.1159/000346898
716

717 Rosen, E.D., Spiegelman, B.M., 2014. What We Talk About When We Talk About
718 Fat. *Cell* 156, 20–44. doi:10.1016/j.cell.2013.12.012
719

720 Sarray, S., Madan, S., Saleh, L.R., Mahmoud, N., Almawi, W.Y., 2015. Validity of
721 adiponectin-to-leptin and adiponectin-to-resistin ratios as predictors of polycystic
722 ovary syndrome. *Fertil. Steril.* 104, 460–466. doi:10.1016/j.fertnstert.2015.05.007
723

724 Seow, K.-M., Tsai, Y.-L., Hwang, J.-L., Hsu, W.-Y., Ho, L.-T., Juan, C.-C., 2009.
725 Omental adipose tissue overexpression of fatty acid transporter CD36 and
726 decreased expression of hormone-sensitive lipase in insulin-resistant women with
727 polycystic ovary syndrome. *Hum. Reprod.* 24, 1982–1988.
728 doi:10.1093/humrep/dep122
729

730 Sepilian, V., Nagamani, M., 2005. Adiponectin levels in women with polycystic ovary
731 syndrome and severe insulin resistance. *J. Soc. Gynecol. Invest.* 12, 129–134.
732 doi:10.1016/j.jsigi.2004.09.003
733

734 Siemienowicz, K., Rae, M.T., Howells, F., Anderson, C., Nicol, L.M., Franks, S.,
735 Duncan, W.C., 2020. Insights into manipulating postprandial energy expenditure to
736 manage weight gain in polycystic ovary syndrome (PCOS). *iScience* 101164.
737 doi:10.1016/j.isci.2020.101164
738

739 Siemienowicz, K.J., Filis, P., Shaw, S., Douglas, A., Thomas, J., Mulroy, S., Howie,
740 F., Fowler, P.A., Duncan, W.C., Rae, M.T., 2019. Fetal androgen exposure is a

741 determinant of adult male metabolic health. *Sci. Rep.* 9, 20195–17.
742 doi:10.1038/s41598-019-56790-4
743
744 Singh, R., Artaza, J.N., Taylor, W.E., Bhasin, S., Gonzalez-Cadavid, N.F., 2003.
745 Androgens stimulate myogenic differentiation and inhibit adipogenesis in C3H
746 10T1/2 pluripotent cells through an androgen receptor-mediated pathway.
747 *Endocrinology* 144, 5081–5088. doi:10.1210/en.2003-0741
748
749 Singh, R., Artaza, J.N., Taylor, W.E., Braga, M., Yuan, X., Gonzalez-Cadavid, N.F.,
750 Bhasin, S., 2005. Testosterone inhibits adipogenic differentiation in 3T3-L1 cells:
751 nuclear translocation of androgen receptor complex with beta-catenin and T-cell
752 factor 4 may bypass canonical Wnt signaling to down-regulate adipogenic
753 transcription factors. *Endocrinology* 147, 141–154. doi:10.1210/en.2004-1649
754
755 Spalding, K.L., Arner, E., Westermark, P.O., Bernard, S., Buchholz, B.A., Bergmann,
756 O., Blomqvist, L., Hoffstedt, J., Näslund, E., Britton, T., Concha, H., Hassan, M.,
757 Rydén, M., Frisén, J., Arner, P., 2008. Dynamics of fat cell turnover in humans.
758 *Nature* 453, 783–787. doi:10.1038/nature06902
759
760 Tchkonina, T., Morbeck, D.E., Zglinicki, von, T., van Deursen, J., Lustgarten, J.,
761 Scrable, H., Khosla, S., Jensen, M.D., Kirkland, J.L., 2010. Fat tissue, aging, and
762 cellular senescence. *Aging Cell* 9, 667–684. doi:10.1111/j.1474-9726.2010.00608.x
763

764 Tchkonina, T., Thomou, T., Zhu, Y., Karagiannides, I., Pothoulakis, C., Jensen, M.D.,
765 Kirkland, J.L., 2013. Mechanisms and Metabolic Implications of Regional Differences
766 among Fat Depots. *Cell Metab.* 17, 644–656. doi:10.1016/j.cmet.2013.03.008
767

768 Teede, H., Deeks, A., Moran, L., 2010. Polycystic ovary syndrome: a complex
769 condition with psychological, reproductive and metabolic manifestations that impacts
770 on health across the lifespan. *BMC Med.* 8, 41. doi:10.1186/1741-7015-8-41
771

772 Veiga-Lopez, A., Moeller, J., Patel, D., Ye, W., Pease, A., Kinns, J., Padmanabhan,
773 V., 2013. Developmental Programming: Impact of Prenatal Testosterone Excess on
774 Insulin Sensitivity, Adiposity, and Free Fatty Acid Profile in Postpubertal Female
775 Sheep. *Endocrinology* 154, 1731–1742. doi:10.1210/en.2012-2145
776

777 Wang, L., Li, S., Zhao, A., Tao, T., Mao, X., Zhang, P., Liu, W., 2012. The
778 expression of sex steroid synthesis and inactivation enzymes in subcutaneous
779 adipose tissue of PCOS patients. *J. Steroid Biochem. Mol. Biol.* 132, 120–126.
780 doi:10.1016/j.jsbmb.2012.02.003
781

782 Weisberg, S.P., McCann, D., Desai, M., Rosenbaum, M., Leibel, R.L., Ferrante,
783 A.W., Jr., 2003. Obesity is associated with macrophage accumulation in adipose
784 tissue. *J. Clin. Invest.* 112, 1796–1808. doi:10.1172/JCI200319246
785

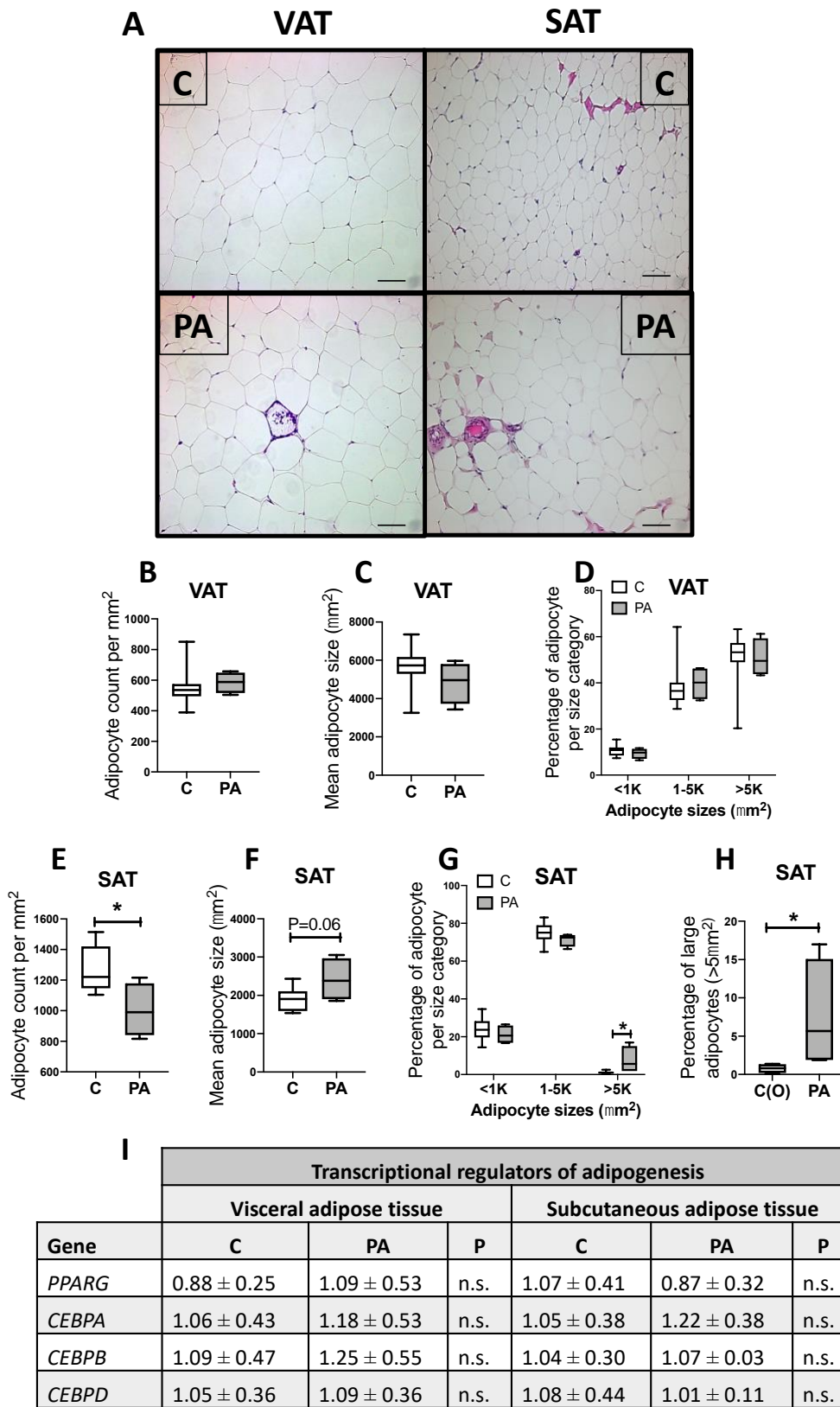
786 Wensvoort, P., 1967. The development of adipose tissue in sheep fetuses.
787 *Path.Vet.* 4, 69–78. doi.org/10.1177/030098586700400107
788

789 Xu, A., Chan, K.W., Hoo, R.L.C., Wang, Y., Tan, K.C.B., Zhang, J., Chen, B., Lam,
790 M.C., Tse, C., Cooper, G.J.S., Lam, K.S.L., 2005. Testosterone selectively reduces
791 the high molecular weight form of adiponectin by inhibiting its secretion from
792 adipocytes. *J. Biol. Chem.* 280, 18073–18080. doi:10.1074/jbc.M414231200
793

794 Yang, X., Jansson, P.-A., Nagaev, I., Jack, M.M., Carvalho, E., Sunnerhagen, K.S.,
795 Cam, M.C., Cushman, S.W., Smith, U., 2004. Evidence of impaired adipogenesis in
796 insulin resistance. *Biochem. Biophys. Res. Commun.* 317, 1045–1051.
797 doi:10.1016/j.bbrc.2004.03.152
798

799 Yildirim, B., Sabir, N., Sabir, Kaleli, B., 2003. Relation of intra-abdominal fat
800 distribution to metabolic disorders in nonobese patients with polycystic ovary
801 syndrome. *Fertil. Steril.* 79, 1358–1364. doi:10.1016/S0015-0282(03)00265-6
802

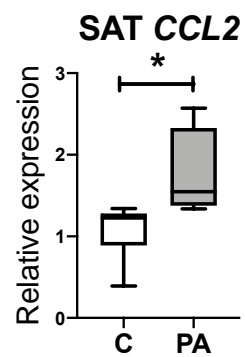
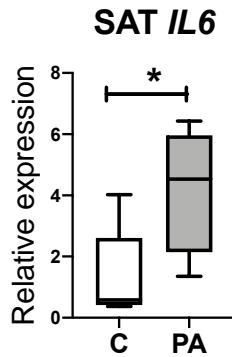
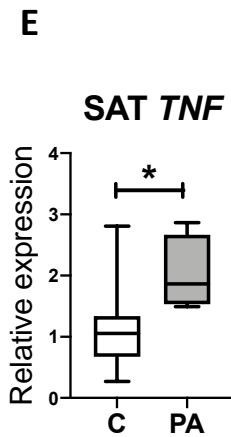
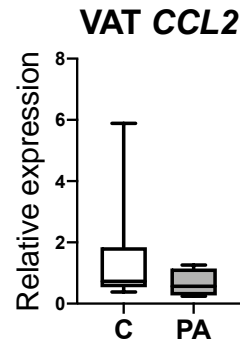
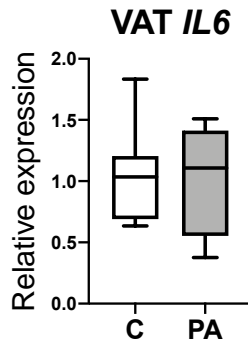
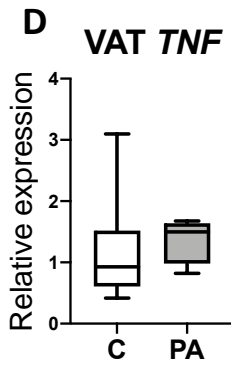
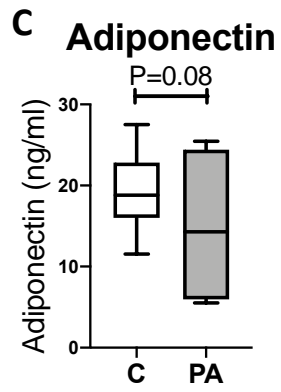
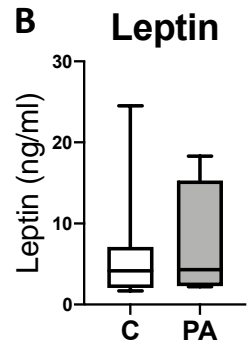
803 Zerradi, M., Dereumetz, J., Boulet, M.-M., Tchernof, A., 2014. Androgens, body fat
804 Distribution and Adipogenesis. *Curr. Obes. Rep.* 3, 396–403. doi:10.1007/s13679-
805 014-0119-6
806



809 **Figure 1.** Adipose tissue analysis in adult (30M) controls (C; n=11) and prenatally
810 androgenised sheep (PA; n=4). **(A)** Histological analysis of adipocyte morphology in
811 VAT and SAT (C=8; PA=4) (scale bars = 100µm). **(B)** In VAT there was no
812 difference in the numbers of adipocytes per mm², **(C)** no difference in the mean size
813 of adipocytes and **(D)** no alteration the number of adipocytes of different sizes. **(E)**
814 PA sheep had decreased number of adipocytes in SAT, **(F)** with a trend to an
815 augmented mean size of adipocytes and **(G)** increased number of large adipocytes.
816 **(H)** The increased number of large SAT adipocytes in PA sheep was still seem when
817 compared to a subset of obese controls (n=4). **(I)** There was no difference in the
818 expression of *PPARG*, *CEBPA*, *CEBPB* and *CEBPD* in adult VAT or SAT. Box plot
819 whiskers are lowest and highest observed values, box is the upper and lower
820 quartile, with median represented by line in box. Data in the table represent mean ±
821 standard deviation. Unpaired, two-tailed Student's t test was used for comparing
822 means of two treatment groups with equal variances accepting $P<0.05$ as significant.
823 (* $P<0.05$).
824

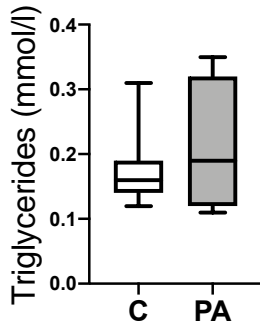
A

Gene	Markers of mature adipocytes		
	Visceral adipose tissue		
Gene	C	PA	P
<i>LEP</i>	1.07 ± 0.39	1.22 ± 0.57	n.s.
<i>ADIPOQ</i>	1.09 ± 0.52	1.56 ± 0.97	n.s.
Gene	Subcutaneous adipose tissue		
<i>LEP</i>	1.07 ± 0.43	1.29 ± 0.50	n.s.
<i>ADIPOQ</i>	1.08 ± 0.46	1.00 ± 0.25	n.s.

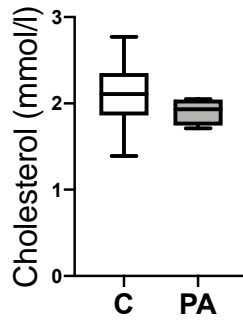


826 **Figure 2.** Adipose tissue function in adult (30M) controls (C; n=11) and prenatally
827 androgenised sheep (PA; n=4). **(A)** There were no differences in *LEP* and *ADIPOQ*
828 expression in VAT or SAT. **(B)** There was no difference in the circulating leptin
829 between controls and PA sheep. **(C)** There was a trend towards decreased
830 adiponectin level in PA sheep. **(D)** There were no differences in transcript
831 abundance of inflammatory markers in VAT. **(E)** In SAT PA sheep had increased
832 *TNF*, *IL6* and *CCL2* when compared to controls. Box plot whiskers are lowest and
833 highest observed values, box is the upper and lower quartile, with median
834 represented by line in box. Data in the table represent mean \pm standard deviation.
835 Unpaired, two-tailed Student's t test was used for comparing means of two treatment
836 groups with equal variances accepting $P < 0.05$ as significant. (* $P < 0.05$).
837

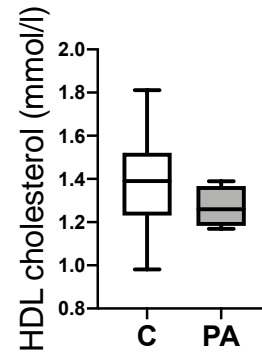
A Triglycerides



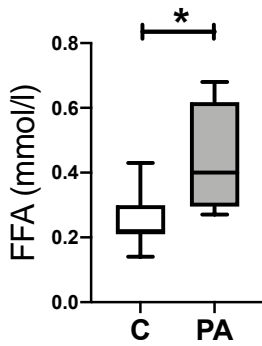
B Total cholesterol



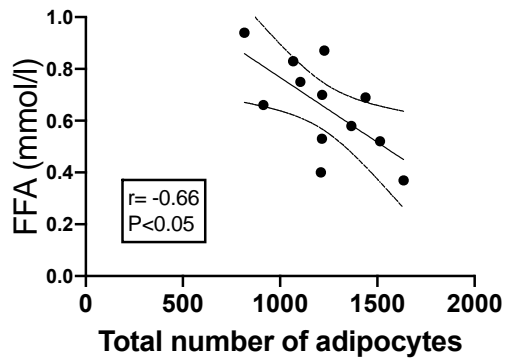
C HDL cholesterol



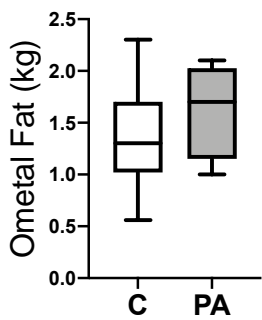
D Free Fatty Acids



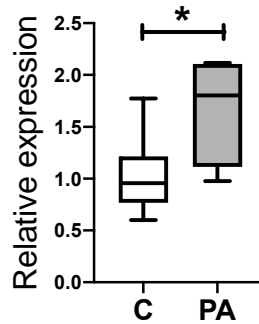
E Total adipocyte number with FFA



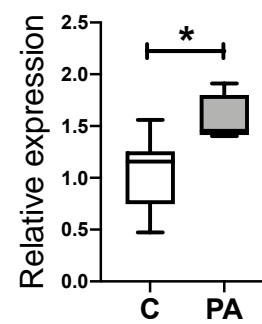
F Omental Fat



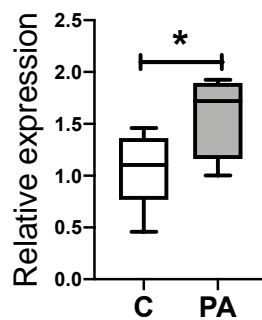
G VAT SLC27A1



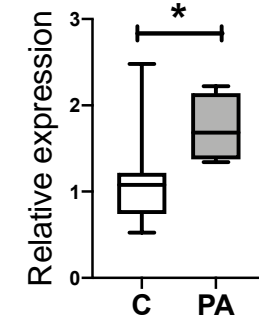
H VAT CAV1



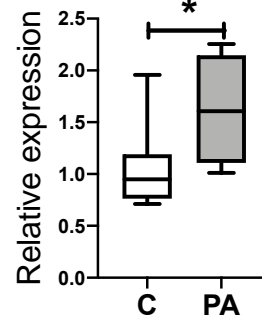
I VAT CAV2



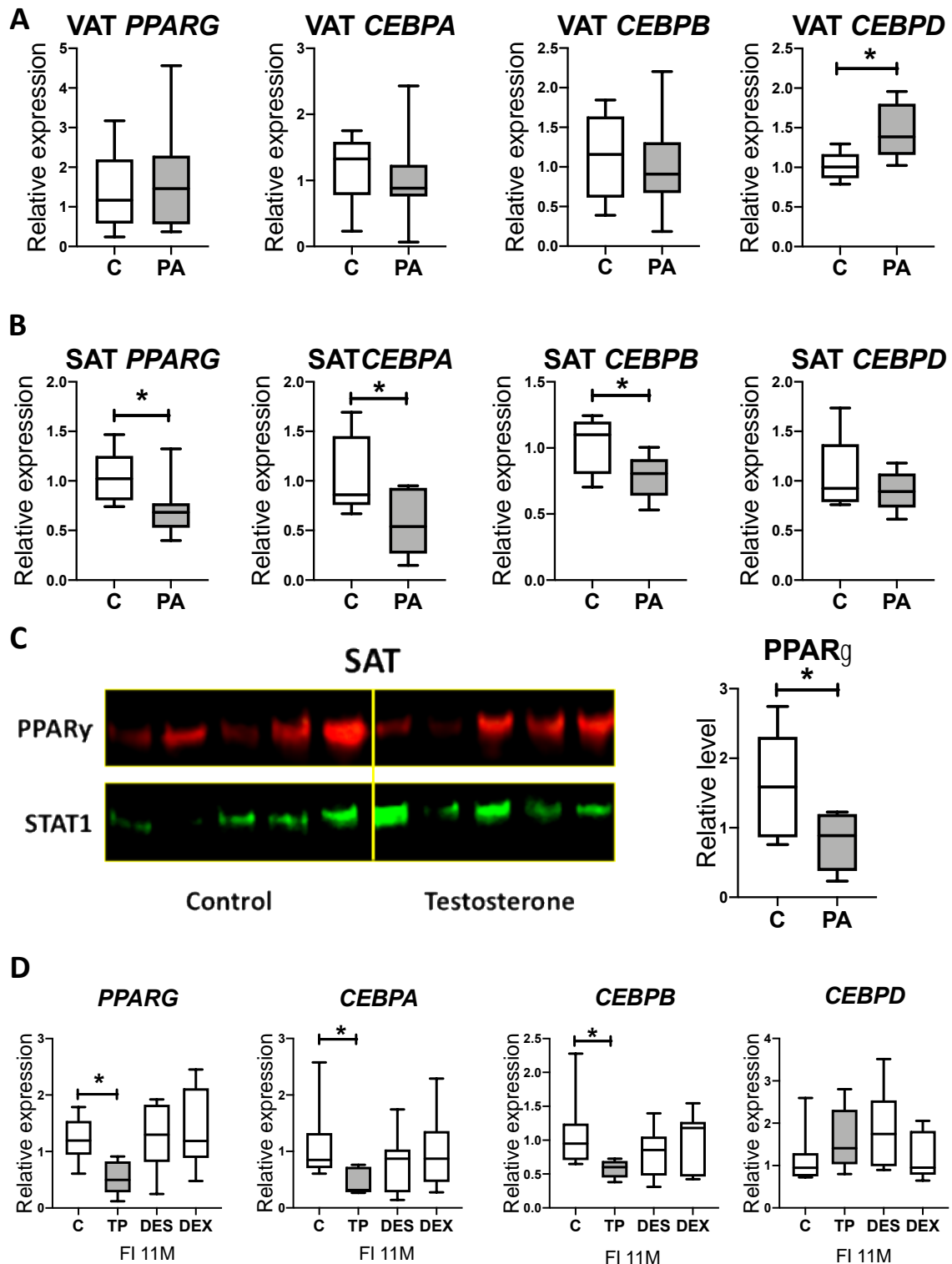
J VAT FABP5



K VAT LPIN2



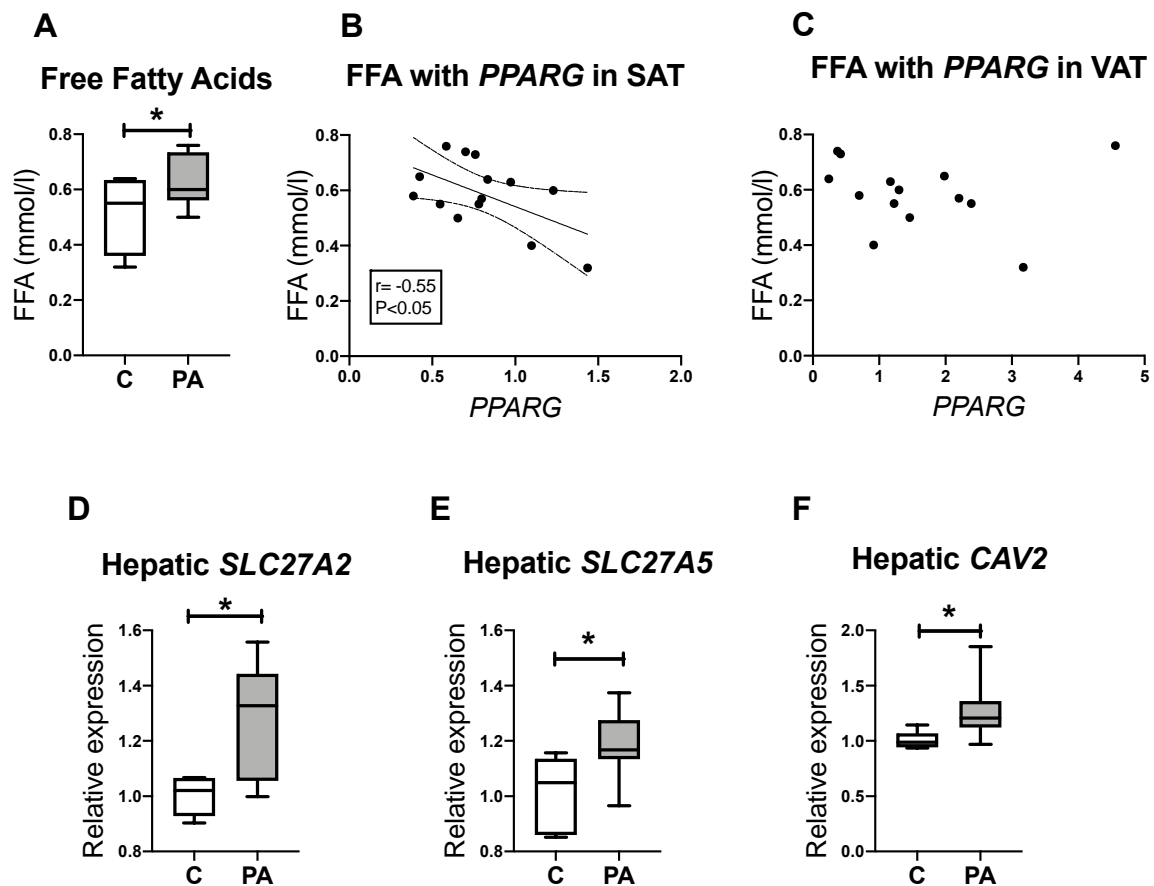
839 **Figure 3.** Metabolic function in adult (30M) controls (C; n=11) and prenatally
840 androgenised sheep (PA; n=4). PCOS-like sheep have normal levels of (A)
841 triglycerides, (B) cholesterol and (C) HDL cholesterol and (D) increased circulating
842 FFAs. (E) There was negative correlation between the total number of adipocytes
843 per mm² and the levels of circulating FFAs. (F) At this time there was no difference in
844 omental fat between controls and PA sheep, however there was increased transcript
845 abundance of genes involved in fat uptake and accumulation in VAT (G) *SLC27A1*,
846 (H) *CAV1*, (I) *CAV2*, (J) *FABP5* and (K) *LPIN2*. Box plot whiskers are lowest and
847 highest observed values, box is the upper and lower quartile, with median
848 represented by line in box. Unpaired, two-tailed Student's t test was used for
849 comparing means of two treatment groups with equal variances accepting $P<0.05$ as
850 significant. Correlation was assessed by calculation of Pearson product-moment co-
851 efficient. (* $P<0.05$).
852



853

854 **Figure 4.** Transcript abundance of adipogenesis markers in adolescent (11M)
 855 controls (C; n=5) and prenatally androgenised sheep (PA; n=9). **(A)** In VAT there
 856 was no difference in the transcript abundance of *PPARG*, *CEBPA* and *CEBPB*,

857 although *CEBPD* was increased. **(B)** Prenatally androgenised sheep had decreased
858 adipogenesis in SAT with a reduction in the transcript abundance of *PPARG*,
859 *CEBPA*, *CEBPB* and no difference in *CEBPD*. **(C)** Decreased level of *PPARG* in
860 SAT in prenatally androgenised females was confirmed with western blot. **(D)**. As
861 compared with controls (C; n=12), the transcript abundance of adipogenesis markers
862 in SAT was decreased by directly injected androgens in fetal life (TP; n=7) but not
863 estrogens (DES; n=8) or glucocorticoids (DEX; n=11). Box plot whiskers are lowest
864 and highest observed values, box is the upper and lower quartile, with median
865 represented by line in box. Unpaired, two-tailed Student's t test was used for
866 comparing means of two treatment groups with equal variances accepting $P < 0.05$ as
867 significant. Unpaired, one-tailed Student's t test was used for western blot analysis.
868 For more than two comparisons ANOVA was used with Dunnett's post hoc test.
869 (* $P < 0.05$; ** $P < 0.01$).
870



871

872

Figure 5. Adipose tissue function in adolescent (11M) controls (C; n=5) and

873

prenatally androgenised sheep (PA; n=9). **(A)** Adolescent prenatally androgenised

874

sheep had increased fasting FFA. **(B)** Concentration of FFAs negatively correlated

875

with *PPARG* ($r=-0.55$) in SAT but not **(C)** with *PPARG* in VAT. There is increased

876

transcript abundance of **(D)** *SLC27A2*, **(E)** *SLC27A5* and **(F)** *CAV2* involved in

877

hepatic fat uptake. Box plot whiskers are lowest and highest observed values, box is

878

the upper and lower quartile, with median represented by line in box. Unpaired, two-

879

tailed Student's t test was used for comparing means of two treatment groups with

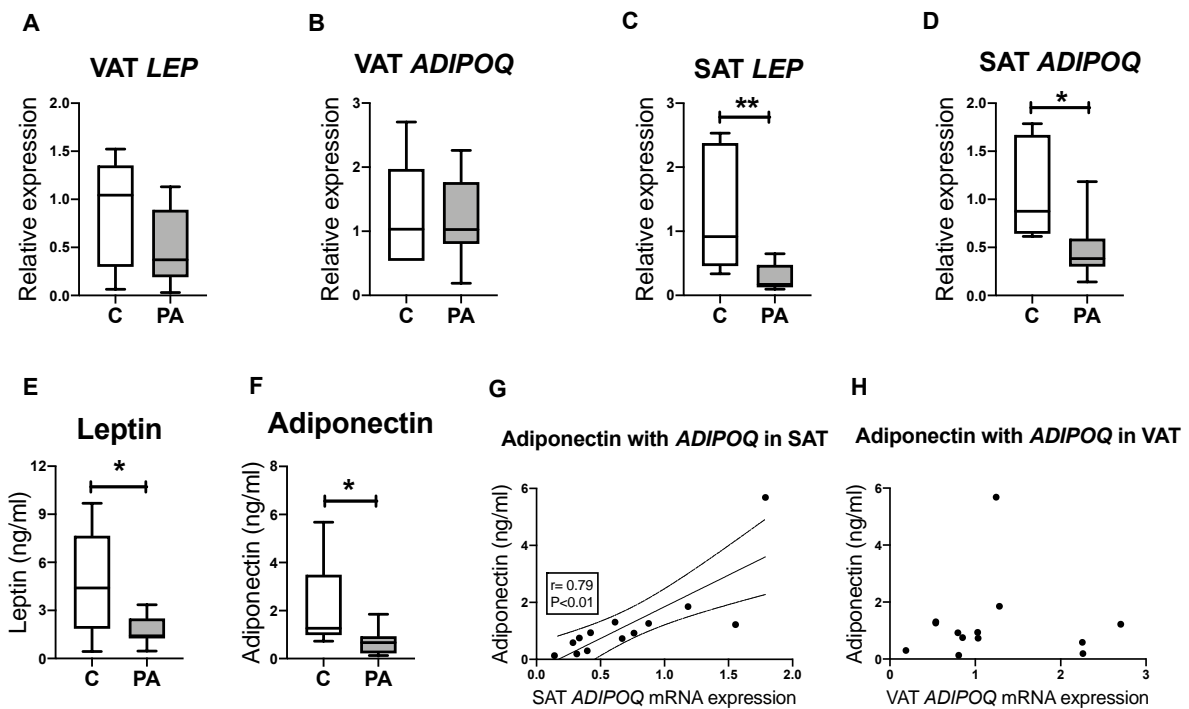
880

equal variances accepting $P<0.05$ as significant. Correlation was assessed by

881

calculation of Pearson product-moment co-efficient. (* $P<0.05$).

882



883

884

Figure 6. Transcript abundance and circulating levels of leptin and adiponectin in

885

adolescent (11M) controls (C; n=5) and prenatally androgenised sheep (PA; n=9). In

886

VAT there was no difference in the expression of (A) *LEP* or (B) *ADIPOQ*.

887

Adolescent prenatally androgenised sheep had decreased expression of (C) *LEP*

888

and (D) *ADIPOQ* in SAT. This was mirrored by a reduction in circulating (E) leptin

889

and (F) adiponectin in PA sheep. (G) Circulating adiponectin correlated ($r=0.79$) with

890

ADIPOQ expression in SAT but not (H) in VAT. Box plot whiskers are lowest and

891

highest observed values, box is the upper and lower quartile, with median

892

represented by line in box. Unpaired, two-tailed Student's t test was used for

893

comparing means of two treatment groups with equal variances accepting $P < 0.05$ as

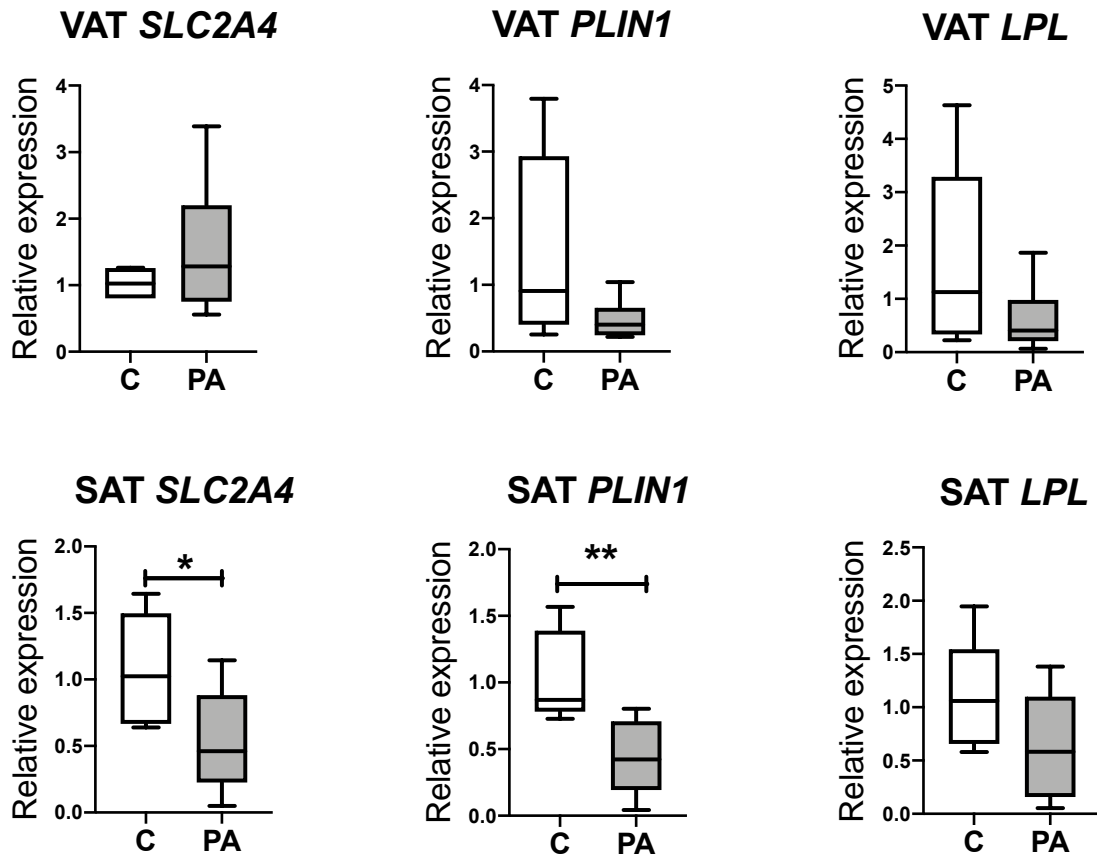
894

significant. Correlation was assessed by calculation of Pearson product-moment co-

895

efficient. (* $P < 0.05$; ** $P < 0.01$).

896



897

898 **Supplementary Figure 1.** Transcript abundance of markers of mature adipocytes in
 899 adolescent (11M) controls (C; n=5) and prenatally androgenised sheep (PA; n=9).

900 (A) In VAT there was no difference in the transcript abundance of *SLC2A4*, *PLIN1*

901 and *LPL*. (B) Prenatally androgenised sheep had decreased expression of *SLC2A4*

902 and *PLIN1* in SAT with no difference in *LPL*. Box plot whiskers are lowest and

903 highest observed values, box is the upper and lower quartile, with median

904 represented by line in box. Unpaired, two-tailed Student's t test was used for

905 comparing means of two treatment groups with equal variances accepting $P < 0.05$ as

906 significant. (* $P < 0.05$; ** $P < 0.01$).

907

908 **Table 1**
 909

Transcriptional regulators of adipogenesis			
Subcutaneous adipose tissue			
Fetal life (D112)			
Gene	C	TP	P
<i>PPARG</i>	1.29 ± 0.85	1.75 ± 0.39	n.s.
<i>CEBPA</i>	1.26 ± 0.79	1.42 ± 0.63	n.s.
<i>CEBPB</i>	1.21 ± 0.72	1.17 ± 0.55	n.s.
<i>CEBPD</i>	1.05 ± 0.35	1.09 ± 0.19	n.s.
Gene	Pre-pubertal (11 weeks)		
<i>PPARG</i>	1.03 ± 0.25	1.30 ± 0.46	n.s.
<i>CEBPA</i>	1.11 ± 0.51	1.47 ± 0.63	n.s.
<i>CEBPB</i>	1.01 ± 0.33	1.34 ± 0.38	n.s.
<i>CEBPD</i>	1.04 ± 0.28	0.90 ± 0.33	n.s.

910

911 **Table 1.** Timing of altered adipogenesis. There was no difference in the expression
 912 of transcription factors involved in adipogenesis in fetal life at GD112 (C; n=9; PA;
 913 n=4) or in pre-pubertal sheep at 11 weeks of age (C; n=8; PA; n=8). Data in the table
 914 represent mean ± standard deviation. Unpaired, two-tailed Student's t test was used
 915 for comparing means of two treatment groups with equal variances accepting $P < 0.05$
 916 as significant.

917

918 **Supplementary Table 1**

Gene	Forward Primer	Reverse Primer
<i>18S</i>	CAACTTTCGATGGTAGTCG	CCTTCCTTGGATGTGGTA
<i>ACTB</i>	ATCGAGGACAGGATGCAGAA	CCAATCCACACGGAGTACTTG
<i>ADIPOQ</i>	AGAGATGGCACCCCTGGT	GACCTTCGATCCCAGTGATT
<i>ADIPOR1</i>	TCTCCTGGCTCTTCCACACT	AGCTCCCCATGATCAGCA
<i>ADIPOR2</i>	AGGTCTGGGAGCCTCTTGTAG	TGAACCCCTCATCTTCCTGA
<i>CAV1</i>	CATCTCTACACTGTTCCCATCC	ACGTCGTCGTTGAGATGCTT
<i>CAV2</i>	CCACAGCAGCGTCGATTAC	CACTGGCTCTGCAATCACAT
<i>CCL2</i>	GACCCCAACCTGAAATGGGT	GCAGTTAGGGGAAGCCAGAA
<i>CEBPA</i>	GTGGACAAGAACAGCAACGA	CGCAGTGTGTCCAGTTCG
<i>CEBPB</i>	GACAAGCACAGCGACGAGTA	AGCTGCTCCACCTTCTTCTG
<i>CEBPD</i>	CGAGTACCGGCAGCGAC	GTCGCGCAGTCCGGC
<i>FABP5</i>	TTCAGCAGCTGGTAGGAAGA	GCACCTACTTTTCGCAGAGC
<i>IL6</i>	AAATGACACCACCCCAAGCA	CTCCAGAAGACCAGCAGTGG
<i>INSR</i>	CACCATCACTCAGGGGAAAC	CAGGAGGTCTCGGAAGTCAG
<i>IRS1</i>	ATCATCAACCCCATCAGACG	GAGTTTGCCACTACCGCTCT
<i>IRS2</i>	TCCAGAACGGCCTCAACTAC	TCAGGTGATGCGTCAAGAAG
<i>LEP</i>	ATCTCACACACGCAGTCCGT	CCAGCAGGTGGAGAAGGTC
<i>LPIN2</i>	GACGTCACCCTGTCACTCTG	GAGTCCAGGGTTTTCTGCAA
<i>MDH1</i>	TTATCTCCGATGGCAACTCC	GGGAGACCTTCAACAACCTTCC
<i>PPARG</i>	TGCAGTGGGGATGTCTCATA	CAGCGGGAAGGACTTTATGT
<i>RPS26</i>	CAAGGTAGTCAGGAATCGCTCT	TTACATGGGCTTTGGTGGAG
<i>SLC27A2</i>	GTGGAAAGGGGAAAATGTGG	TCAAATTCATGGTCTGCCTTC
<i>SLC27A5</i>	CGGACATCAAGTTGCGAAG	ATCCCTGATACCTGCAGCAC
<i>SLC2A4</i>	CCAGCATCTTTGAGTCAGCA	CAGAAGCAGAGCCACAGTCA
<i>TNF</i>	GGTGCCTCAGCCTCTTCT	GAACCAGAGGCCTGTTGAAG

919

920 **Supplementary Table 1.** Primers for real-time RT-PCR analysis. Forward and
921 reverse primers were designed using Primer3 Input version 0.4 online software
922 (<http://frodo.wi.mit.edu>) with DNA sequences obtained at Ensembl Genome Browser.
923 To confirm the validity of the gene product in the sheep, both conventional PCR and
924 amplicon sequencing were performed. Primer specificity and efficacy for qRT-PCR
925 was evaluated through the generation of standard curves with serial dilutions of

926 cDNA; a standard curve slope of approximately -3.3 was accepted as efficient, and a
927 melt-curve analysis was also performed.